Geophysical Research Letters

RESEARCH LETTER
10.1029/2019GL081998

Electron Sublayers and the Associated Magnetic Topologies in the Inner Low-Latitude Boundary Layer

X.-C. Dong[1], M. W. Dunlop[1,2], K. J. Trattner[3], T.-Y. Wang[2], Z. Y. Pu[4], J.-S. Zhao[5], J.-B. Cao[1], Barbara Giles[6], and C. T. Russell[7]

[1]School of Space and Environment, Beihang University, Beijing, China, [2]RAL Space, STFC, Oxfordshire, UK, [3]LASP, University of Colorado Boulder, Boulder, CO, USA, [4]School of Earth and Space Sciences, Peking University, Beijing, China, [5]Key Laboratory of Planetary Sciences, Purple Mountain Observatory, Chinese Academy of Sciences, Nanjing, China, [6]NASA Goddard Space Flight Center, Greenbelt, MD, USA, [7]Department of Earth, Planetary and Space Sciences, UCLA, Los Angeles, CA, USA

Key Points:
- Observational results show that the inner LLBL contains multiple electron sublayers, which are more complex than previous results
- These sublayers include three different magnetic field line topologies
- The study reports evidence in the LLBL that high- and low-latitude magnetic reconnection can happen simultaneously under southward IMF

Supporting Information:
- Supporting Information S1

Correspondence to:
M. W. Dunlop,
malcolm.dunlop@stfc.ac.uk

Citation:
Dong, X.-C., Dunlop, M. W., Trattner, K. J., Wang, T.-Y., Pu, Z. Y., Zhao, J.-S., et al. (2019). Electron sublayers and the associated magnetic topologies in the inner low-latitude boundary layer. *Geophysical Research Letters*, *46*, 5746–5753. https://doi.org/10.1029/2019GL081998

Received 10 JAN 2019
Accepted 22 MAY 2019
Accepted article online 29 MAY 2019
Published online 13 JUN 2019

Abstract The low-latitude boundary layer (LLBL) plays an important role as a transition layer in coupling the magnetosheath and magnetosphere. Using high-resolution Magnetospheric Multiscale data, we analyze the electron distributions in the inner region of the LLBL, during an active period of magnetic reconnection under southward interplanetary magnetic field. According to the measured electron energy anisotropy, we suggest that this inner LLBL can be divided into six sublayers corresponding to three types of magnetic field-line topologies: (1) open magnetic field line topology from magnetosheath to southern magnetosphere, (2) open magnetic field line topology from magnetosheath to northern magnetosphere, and (3) reclosed magnetic field line topology. These different scenarios indicate that magnetic reconnection occurs at both northern and southern locations of the spacecraft and thus suggest that magnetic reconnection was active simultaneously at high and low latitude on the magnetopause, equatorward of the cusps. These results provide evidence within the LLBL for such multiple X-line formation.

Plain Language Summary Magnetic reconnection is a fundamental energy conversion process in space, astrophysical, and laboratorial plasmas. At the Earth's magnetopause, the occurrence and location of magnetic reconnection are of particular interest. By analyzing the detailed sublayers of the inner low-latitude boundary layer, we identified different magnetic field-line topologies. The different field line topologies indicate that magnetic reconnection happens both north and south of the spacecraft and thus suggest that magnetic reconnection was active at both the high- and low-latitude dayside magnetopause. These results provide further evidence for large-scale multiple X-line formation.

1. Introduction

The low-latitude boundary layer (LLBL), which contains a mixture of magnetosheath and magnetospheric plasma populations, is often observed immediately earthward of the magnetopause (Eastman et al., 1976; Sckopke et al., 1981). The LLBL is a transition layer between the magnetosheath and magnetosphere and thus plays an important role in the coupling between the solar wind and magnetosphere (e.g., Bogdanova et al., 2006, 2008; Cai et al., 2009; Dunlop et al., 2008; Hasegawa et al., 2009; Zhang et al., 2012).

Several mechanisms have been proposed to explain the formation of the LLBL, including: magnetic reconnection (Gosling et al., 1990); plasma diffusion (Mitchell et al., 1987; Sonnerup, 1980), and the Kelvin-Helmholtz instability (Hasegawa et al., 2004; Ogilvie & Fitzenreiter, 1989). It is generally accepted, however, that the diffusion coefficients corresponding to wave instabilities and turbulence are not enough to cause the majority of a thick LLBL (Bauer et al., 2001; Treumann et al., 1995). The Kelvin-Helmholtz instability occurs predominantly on the flank sides of the magnetosphere and thus cannot explain the formation of the LLBL near the subsolar region. The remaining formation mechanism, magnetic reconnection, occurs between magnetosheath and terrestrial field lines, during which the open magnetic field created threads the magnetopause. Figure 1 shows a simplified, 2-D schematic view of a LLBL created by magnetic reconnection. The magnetosheath and magnetosphere are located on the left and right sides, respectively (grey lines). In this simple scenario, magnetic field lines have reconnected in the middle region and subsequently move downstream through the operation of magnetic tension and plasma convection. A boundary layer is created during this process (the region surrounded by black magnetic field lines) and can be divided into two regions by

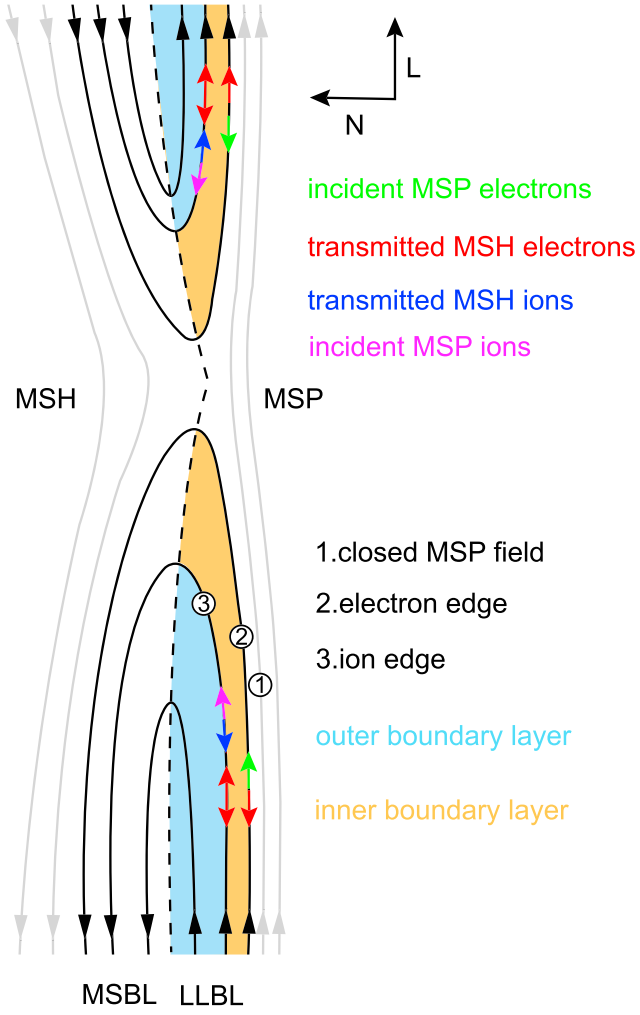

Figure 1. Sketch illustrating the low-latitude boundary layer (LLBL) created by magnetic reconnection. Magnetic reconnection happens in the center region. The dashed line is the magnetopause current layer, which divides the reconnection boundary layer into magnetosheath boundary layer (MSBL) and LLBL. Field line 1 is the closed magnetospheric magnetic field. Field line 2 is the first opened field line with transmitted magnetosheath (single red arrow) and incident magnetospheric (single green arrow) electrons. It is termed as the electron edge. Field line 3 is an older reconnected line where the transmitted magnetosheath ions arrive (single blue arrow) and transmitted magnetosheath electrons become balanced due to their mirror from ionosphere and is termed as the ion edge. The region with both magnetosheath and magnetospheric electrons is inner boundary layer (yellow region).

the magnetopause current layer (dashed line). The left side of boundary is usually referred to as the magnetosheath boundary layer (MSBL), and the right shaded region is called LLBL. In the LLBL, the field line labeled "2" is the most recently reconnected field line and therefore forms the separatrix, or boundary between closed and open field lines. Along field line 2, magnetosheath electrons (red arrows) will arrive at any crossing point first due to their fast velocity and magnetospheric electrons (green arrows) will escape on the newly opened field line and be lost. This is therefore termed as the LLBL electron edge (Gosling et al., 1990). Field-line 3 represents one of the older reconnected field lines where magnetosheath ions have first arrived (blue arrows) and is therefore termed as the LLBL ion edge. The separation between the electron and ion edge is due to time-of-flight effect between the most energetic ions and electrons. Furthermore, at the ion edge, the transmitted electrons will have time to return from their ionosphere mirror point and therefore begin to form a counterstreaming distribution (red double arrows) near the ion edge. Thus, in this scenario, if a spacecraft is initially located in the magnetosphere and then crosses the LLBL from the upper (lower) side of the magnetic reconnection region, the parallel (antiparallel) transmitted magnetosheath electrons and antiparallel (parallel) incident MSP electrons will first be observed during the encounter with the electron edge. Following this, the transmitted ions would be observed at locations starting from the ion edge and transmitted electrons will become counterstreaming.

Using the above features, we can determine the magnetic field topology by analyzing changes in the electron distributions. Øieroset et al. (2015) examined the electron distribution covering the entire energy range in the magnetosheath and magnetospheric layers to determine the magnetic field topology in the whole LLBL. This method is also used to determine the magnetic field topology of different scale flux transfer events (Dong et al., 2017; Lv et al., 2016; Pu et al., 2013; Zhong et al., 2013).

At the magnetopause, reconnection is often discussed in terms of two general types: antiparallel and component reconnection. Antiparallel reconnection occurs where the shocked magnetosheath and magnetospheric magnetic field have essentially opposite polarity, while component reconnection is assumed to occur during a wide range of shear angles (Trattner et al., 2007a, 2007b). A well-localized antiparallel region exists on the magnetopause during any interplanetary magnetic field (IMF) direction. It is understood that component reconnection most often is limited to occur near the subsolar region, along a tilted X-line across the subsolar point when the IMF is southward (Cooling et al., 2001; Sonnerup, 1974; Trenchi et al., 2008). When the IMF is northward, antiparallel reconnection dominates poleward of the magnetospheric cusps as is confirmed by many observations (e.g., Fuselier et al., 2014; Trattner et al., 2004; Zhang et al., 2008). For southward IMF, component reconnection at low latitude has been studied widely (e.g., Burch & Phan, 2016; Dunlop, Zhang, Bogdanova, Trattner, et al., 2011; Dunlop, Zhang, Bogdanova, Lockwood, et al., 2011; Khotyaintsev et al., 2016). Whether low-latitude component reconnection and higher-latitude antiparallel reconnection (south of the cusps) can occur simultaneously under southward IMF, however, is still an issue which needs further clarification. The statistical results on reconnection jets of Pu et al. (2007) give an indirect evidence that both antiparallel and component magnetic reconnection may occur at the magnetopause under dusk-dawn IMF orientation. During southward and B_Y-dominated IMF conditions, Dunlop et al. (2009) reported high-latitude reconnection equatorward of the cusp in the region where the Earth's and the magnetosheath magnetic fields were antiparallel. Evidence for large-scale multiple reconnection sites

has also been presented using observations in the MSBL and cusp region (Fuselier et al., 2011, 2018; Trattner et al., 2012). It has not been clear, however, how the plasma distribution and magnetic topology in the LLBL are affected when multiple reconnection sites are present. One might expect that the simple ion-electron edge picture shown in Figure 1, and which is described above, would be significantly altered in the presence of multiple reconnection sites, since contributions from two reconnection sites, for example, affect the distributions.

The LLBL often exhibits two substructures, which include the outer boundary layer (OBL) and inner boundary layer (IBL). The OBL is dominated by magnetosheath particles, whereas the IBL includes both magnetosheath and magnetospheric particles (Bauer et al., 2001; Hasegawa et al., 2009; Le et al., 1996; Song et al., 1990). However, signatures for the ion and electron populations may be different. In this paper we define IBL as a region between the electron and ion edge and containing both magnetosheath and magnetospheric electrons (yellow region in Figure 1).

Typical spacecraft crossings through the IBL are fast (~20 s, e.g., Phan et al., 1996), and this region was therefore often not well resolved prior to Magnetospheric Multiscale (MMS). In this paper, we use data from the National Aeronautics and Space Administration MMS mission (Burch et al., 2015), which launched four spacecraft, closely spaced in order to study the small-scale physical process. MMS provides unprecedented higher resolution plasma data. Using MMS data, we analyze the detailed plasma distribution and small-scale sublayers of the IBL.

2. Data Set and Event Study

The high-resolution plasma data (30-ms cadence for electron and 150 ms for ion) from the fast plasma investigation (Pollock et al., 2016) and the magnetic field data from the Fluxgate Magnetometer (Russell et al., 2016) are used. All vector data are given in geocentric solar magnetospheric (GSM) coordinate system.

We investigate the magnetopause crossing observed on 13 November 2015 around 04:02:30 where Figure 2 shows an overview of this event. During this time, MMS is located near [10.6, 0.5, -0.7] R_E (Earth radius) in GSM coordinates (Figures 2a and 2b) and crossed from the magnetosphere to the magnetosheath. The spacecraft are located in the magnetospheric region before 04:02:06 UT (before the shaded region), characterized by steady northward magnetic field (Figure 2a), low plasma density (Figure 2b), high temperature (Figure 2c), a population of energetic (core energy of ~10 keV for electrons and ~20 keV for ions) magnetospheric plasmas, a population of cold (<30 eV for electrons and ~40 eV for ions) magnetospheric plasmas, and a lack of broadband low-energy magnetosheath plasmas (Figures 2g and 2h). During 04:02:06-04:02:12 UT (shaded region), the increase of magnetosheath energy electrons (30-300 eV; green curve in Figure 2d) and the accompanying decrease of magnetospheric energy electrons (red curve in Figure 2d) indicate the existence of open magnetic field lines. We define this region as the IBL, and it will be investigated in detail later. After the IBL (04:02:12.22 UT), magnetospheric electrons have almost disappeared and the density of transmitted magnetosheath electrons was ~3 cm^{-3} (Figures 2d and 2h). The broadband magnetosheath energy ions have appeared (Figure 2g), and the ion velocity begins to increase up to 250 km/s in the southeast direction (Figure 2f); consistent with crossing through a reconnection jet, which originates at an X-line northward of the spacecraft. The radial separation between the first arrival of transmitted electrons and ions is consistent with time-of-flight effect in the magnetic reconnection boundary layer.

During 04:02:41-04:02:49 UT (around the right dashed line), the magnetic field rotation from northward to southward represent the magnetopause current sheet. The region between the IBL and the current sheet is the OBL of the LLBL. The ion population in the ion jet (04:02:19.166-04:02:19.316 UT; see the 2-D ion distribution in Figure 2l) is consistent with previous predictions and observations of the velocity distributions of the outflows of magnetic reconnection ("D-shaped" distribution; Cao et al., 2013; Cowley, 1982), as a result of magnetosheath ions transmitted through the current sheet and injected cold magnetospheric ions. The above ion velocity and distribution features indicate that magnetic reconnection occurred northward of the spacecraft. After the current sheet, the spacecraft enter the MSBL and magnetosheath region, characterized by dense (~20 cm^{-3}) and cold plasma.

The inset in Figures 2i-2k shows the electron energy spectrograms for electrons directed parallel (0-30°) and antiparallel (150-180°) to the magnetic field and the logarithmic ratio of them in the IBL from 04:02:03 to

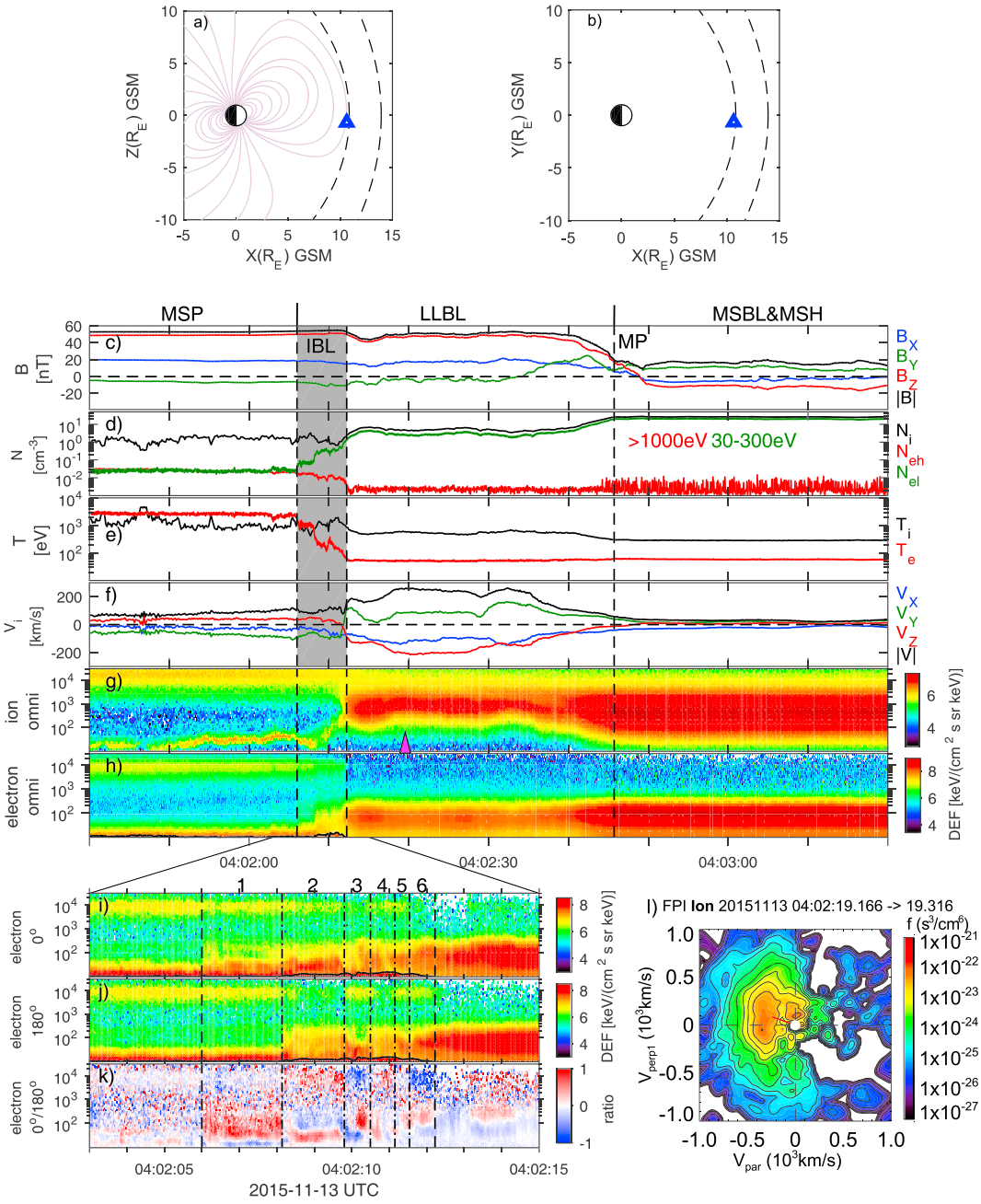

Figure 2. MMS1 observation of the magnetopause crossing event. The panels show (a and b) MMS location in the geocentric solar magnetospheric (GSM) coordinates, (c) magnitude and component of magnetic field (GSM), (d) the ion density and the electron density of the high energy and low energy, (e) the temperature of ion and electron larger than 30 eV, (f) magnitude and component of ion velocity (GSM), and (g and h) the ion and electron spectrograms of differential energy flux. (i-k) Detailed electron distribution of inner boundary layer (shaded region), (i and j) electron spectrograms of differential energy flux in the parallel and antiparallel directions, and (k) the logarithmic ratio of parallel and antiparallel electron differential energy fluxes. The black lines on the bottom of h-j are the spacecraft potential, below which are the photoelectrons. (l) Two-dimensional cuts through the 3-D ion velocity distributions obtained in the southward ion jet (magenta arrow). The shaded region is divided into six regions by dash-dotted line according to electron parallel-to-antiparallel anisotropy.

04:02:15 UT. The IBL has been divided into six regions by dash-dotted lines according to different parallel-to-antiparallel anisotropy of electrons (Figure 2k). The four spacecraft timing method has been used during the magnetic field rotation around 04:02:12UT and produces a propagation speed of 50×[-0.93, 0.20, 0.31] km/s.

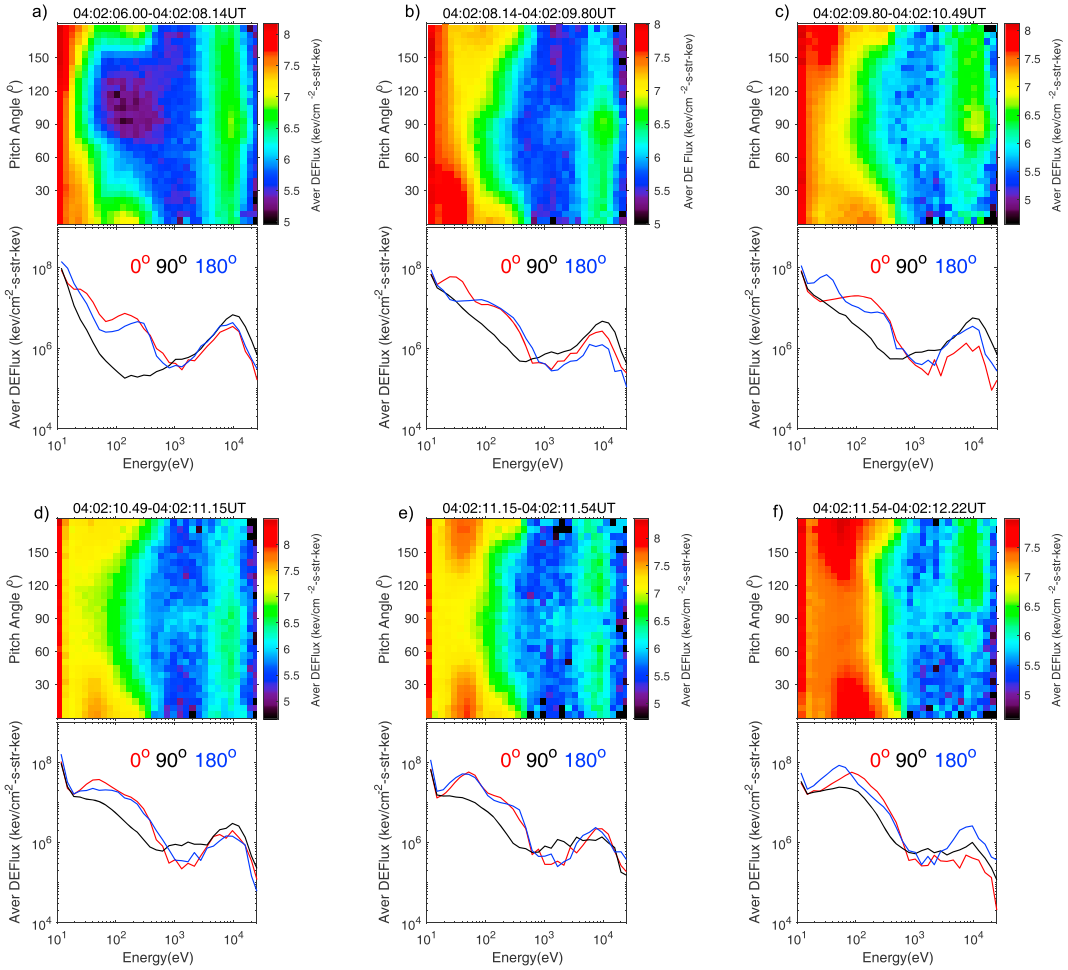

Figure 3. The average electron pitch angle distributions as a function of differential energy flux (upper panels) and energy spectra (lower panel) for each of the six regions in Figure 2. The energy spectra are for pitch angle of 0, 90, and 180°, respectively. (a-f) Regions 1-6 in Figure 2.

Assuming the spacecraft have crossed the LLBL at this constant speed, we can thus estimate of the width of region 1 to region 6 as 107, 83, 34.5, 33, 15, and 34 km, respectively. For comparison, the gyroradius of the magnetospheric ions and electrons in this region are 377 and 6.3 km (using 2×10^4 eV for ions and 1×10^4 eV for electrons). Therefore, the widths of these regions are all comparable to subion scales and the smallest one even approaches the electron scale. Figure 3 shows the average differential energy flux as a function of pitch angle and energy spectra for each of the six time intervals marked in Figures 2i-2k. We can interpret the electron distribution anisotropy using Figures 2i-2k, in conjunction with detailed pitch angle distribution and energy spectra in Figure 3, as described below.

Figures 2i-2k show that in the magnetosphere just before the IBL, both the cold (<30 eV) and energetic (~10 keV) magnetospheric electron populations are nearly balanced at 0 and 180° degrees pitch angles, indicating that these are on closed magnetic field lines. When the spacecraft encounter the IBL, three electron populations are observed (Figures 2i-2k and 3): a population of magnetospheric cold or slighted heated (<50 eV) electrons, a population of magnetosheath (core energy of 50 eV) electrons, and a population of energetic, magnetospheric (core energy of 10 keV) electrons (here the terms “magnetospheric” and “magnetosheath” imply the likely origin of these populations). The distributions show that six distinct electron distributions are observed: Region (1) contains almost isotropic magnetospheric energetic electrons, low-density parallel magnetosheath electrons, and parallel magnetospheric cold electrons (Figure 3a); Region (2) contains parallel energetic magnetospheric electrons, antiparallel magnetosheath electrons, and parallel magnetospheric cold electrons (Figure 3b); Region (3) contains antiparallel energetic magnetospheric electrons, parallel magnetosheath electrons, and antiparallel magnetospheric cold electrons (Figure 3c); Region (4) contains

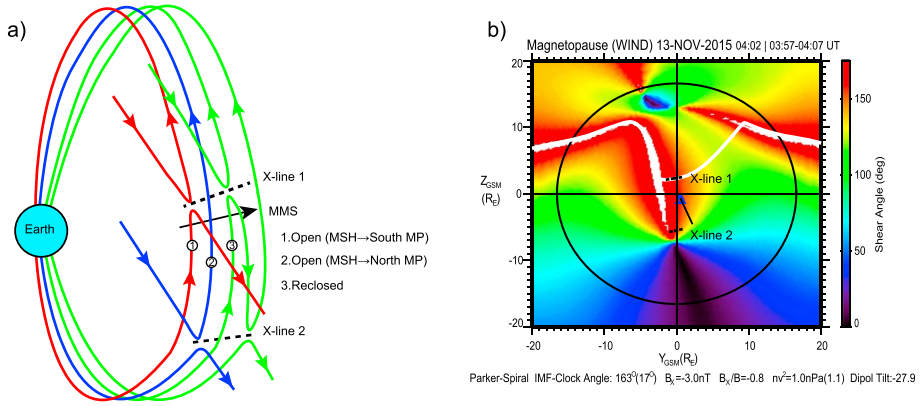

Figure 4. (a) Schematic showing a possible 3-D configuration of magnetic topologies. The circled numbers represent three different magnetic topologies mentioned above. The black arrow line is the trajectory of Magnetospheric Multiscale (MMS), which crossed all of these topologies. The two dashed line is the predicted reconnection regions in low and high latitudes. (b) The magnetopause shear angle seen from the Sun with the predicted reconnection and MMS locations at the magnetopause. The predicted two reconnection regions in this event are also noted.

more parallel energetic magnetospheric electrons and nearly bistreaming magnetosheath electrons with a little higher flux in parallel direction (Figure 3d); Region (5) contains both nearly isotropic magnetospheric and bistreaming magnetosheath electrons (Figure 3e); Region (6) contains antiparallel energetic magnetospheric electrons and bistreaming magnetosheath electrons, which were slightly accelerated in the parallel direction (Figure 3f).

These distributions imply distinct field line geometry. The essentially balanced energetic magnetospheric electrons at 0 and 180° pitch angles in Regions 1 and 5 suggest closed field-line geometry, while the different distributions of magnetosheath electrons (parallel in Region 1 and bistreaming in Region 5) may suggest that field lines in Region 1 have been recently reclosed and the magnetosheath electrons at that location have not had time to become balanced. The essentially parallel (antiparallel) high-energy magnetospheric electrons in Regions 2 and 4 (Regions 3 and 6) suggest an open field-line geometry connecting the southern (northern) magnetosphere to the magnetosheath. In addition, the antiparallel (parallel) magnetosheath electrons and parallel (antiparallel) magnetospheric cold electrons in Region 2 (Region 3) are typical of recently opened field-line geometry, which corresponds to active reconnection. Finally, the more balanced low-energy electron distribution in Regions 4 and 6 may result from the mirroring at the low-altitude ionosphere. This sequence is therefore more complex than that which is expected from a simple, single X-line topology and we will discuss this below.

3. Summary and Discussion

We have investigated the detailed electron distribution of the inner LLBL (IBL) observed by MMS during southward IMF conditions. The high-speed ion jet, "D-shaped" ion distribution and separation between the ion and electron edge indicate that this LLBL is created by magnetic reconnection. Observational results show that the IBL can be divided into six sublayers characterized by their different electron distributions. We find that three kinds of magnetic field topologies are included: (1) open field lines connecting to the southern magnetosphere, (2) open field lines connecting to northern magnetosphere, and (3) reclosed field lines connecting to both hemispheres. Furthermore, the distributions of transmitted magnetosheath electrons indicate that recently opened field lines are included in these two kinds of open field line geometry, corresponding to an interval of active reconnection.

The coexistence of the above three field line topologies cannot be explained by a single X-line reconnection picture and indicates that reconnection X-lines were present both north and south of the spacecraft. Since we do not observe any typical characteristics of FTEs, such as bipolar B_N and enhancement of the core field, we suggest that the distance between the two reconnection sites is much larger than the typical FTE scale (1-2 R_E). Ion signatures from the reconnection site southward of the spacecraft were not observed, which may

indicate that this reconnection site was located far from the spacecraft (Hasegawa et al., 2009). Thus, the observations suggest that both low-latitude reconnection and higher-latitude reconnection happened simultaneously, but farther away from each other than for a typical FTE. Figure 4a shows a possible 3-D configuration of magnetic topologies for the event. The open field line 1 from the southern magnetosphere to the magnetosheath is created by low-latitude reconnection and that of field line 2 (connecting from the magnetosheath to the northern magnetosphere) by reconnection in the southern hemisphere at higher latitude. The reclosed field line 3 is created by both reconnection sites.

Our interpretation is supported by the maximum magnetic shear model (Figure 4b; Trattner et al., 2007a, 2007b). The predicted component reconnection region is located northward of the spacecraft (X-line 1), consistent with the observed southward directed ion jet. The antiparallel reconnection region extends from the northern hemisphere to the southern high-latitude region. Thus, reconnection is predicted to occur southward of the spacecraft at high latitudes, in agreement with the second X-line (X-line 2) inferred from the observations.

The MMS observations from the inner LLBL presented in this paper provide evidence that high- and low-latitude magnetic reconnection were simultaneously active at the magnetopause equatorward of the cusps. Such events may not be uncommon. Two similar events are presented in Figure S1 in the supporting information and will be fully investigated in our future work. Finally, we can estimate the reconnection rate at the low- and high-latitude reconnection locations, respectively, using the estimated spatial size (width) of each sublayer, together with the nearly constant magnetic field. We find that the magnetic flux created by low-latitude reconnection is approximately 25% higher than that of the high-latitude reconnection site. This suggests that both reconnection sites were important for the LLBL formation for this event.

Acknowledgments
For MMS data visit https://lasp.colorado.edu/mms/sdc/public/. We thank the entire MMS team and instrument PIs for data access and support. M. W. Dunlop is partly supported by an STFC in-house research grant ST/M001083/1 and is supported by the NSFC grants 41574155 and 41431071, and the NERC grant NE/P016863/1.

References

Bauer, T. M., Treumann, R. A., & Baumjohann, W. (2001). Investigation of the outer and inner low-latitude boundary layers. *Annales de Geophysique*, *19*(9), 1065–1088. https://doi.org/10.5194/angeo-19-1065-2001

Bogdanova, Y. V., Owen, C. J., Fazakerley, A. N., Klecker, B., & Reme, H. (2006). Statistical study of the location and size of the electron edge of the low-latitude boundary layer as observed by Cluster at mid-altitudes. *Annales de Geophysique*, *24*(10), 2645–2665. https://doi.org/10.5194/angeo-24-2645-2006

Bogdanova, Y. V., Owen, C. J., Dunlop, M. W., Wild, J. A., Davies, J. A., Lahiff, A. D., et al. (2008). Formation of the low-latitude boundary layer and cusp under the northward IMF: Simultaneous observations by Cluster and Double Star. *Journal of Geophysical Research*, *113*, A07S07. https://doi.org/10.1029/2007JA012762

Burch, J. L., Moore, T. E., Torbert, R. B., & Giles, B. L. (2015). Magnetospheric Multiscale overview and science objectives. *Space Science Reviews*, *199*(1–4), 5–21. https://doi.org/10.1007/s11214-015-0164-9

Burch, J. L., & Phan, T. D. (2016). Magnetic reconnection at the dayside magnetopause: Advances with MMS. *Geophysical Research Letters*, *43*, 8327–8338. https://doi.org/10.1002/2016GL069787

Cai, C. L., Dandouras, I., Rème, H., Cao, J. B., Zhou, G. C., Shen, C., et al. (2009). Magnetosheath excursion and the relevant transport process at the magnetopause. *Annales Geophysicae*, *27*(8), 2997–3005. https://doi.org/10.5194/angeo-27-2997-2009

Cao, J., Ma, Y., Parks, G., Reme, H., Dandouras, I., & Zhang, T. (2013). Kinetic analysis of the energy transport of bursty bulk flows in the plasma sheet. *Journal of Geophysical Research: Space Physics*, *118*, 313–320. https://doi.org/10.1029/2012JA018351

Cooling, B. M. A., Owen, C. J., & Schwartz, S. J. (2001). Role of the magnetosheath flow in determining the motion of open flux tubes. *Journal of Geophysical Research*, *106*(A9), 18,763–18,775. https://doi.org/10.1029/2000JA000455

Cowley, S. W. H. (1982). The causes of convection in the Earth's magnetosphere: A review of developments during the IMS. *Reviews of Geophysics*, *20*, 531–565. https://doi.org/10.1029/RG020i003p00531

Dong, X.-C., Dunlop, M. W., Trattner, K. J., Phan, T. D., Fu, H. S., Cao, J. B., et al. (2017). Structure and evolution of flux transfer events near dayside magnetic reconnection dissipation region: MMS observations. *Geophysical Research Letters*, *44*, 5951–5959. https://doi.org/10.1002/2017GL073411

Dunlop, M. W., Zhang, Q. H., Bogdanova, Y. V., Lockwood, M., Pu, Z., Hasegawa, H., et al. (2011). Extended magnetic reconnection across the dayside magnetopause. *Physical Review Letters*, *107*(2), 025004. https://doi.org/10.1103/PhysRevLett.107.025004

Dunlop, M. W., Zhang, Q. H., Bogdanova, Y. V., Trattner, K. J., Pu, Z., Hasegawa, H., et al. (2011). Magnetopause reconnection across wide local time. *Annales Geophysicae*, *29*(9), 1683–1697. https://doi.org/10.5194/angeo-29-1683-201

Dunlop, M. W., Zhang, Q. H., Xiao, C. J., He, J. S., Pu, Z., Fear, R. C., et al. (2009). Reconnection at high latitudes: Antiparallel merging. *Physical Review Letters*, *102*(7). https://doi.org/10.1103/PhysRevLett.102.075005

Dunlop, M. W., Taylor, M. G. G. T., Bogdanova, Y. V., Shen, C., Pitout, F., Pu, Z., et al. (2008). Electron structure of the magnetopause boundary layer: Cluster/Double Star observations. *Journal of Geophysical Research*, *113*, A07S19. https://doi.org/10.1029/2007JA012788

Eastman, T. E., Hones, E. W. Jr., Bame, S. J., & Asbridge, J. R. (1976). The magnetospheric boundary layer: Site of plasma, momentum and energy transfer from the magnetosheath into the magnetosphere. *Geophysical Research Letters*, *3*(11), 685–688. https://doi.org/10.1029/GL003i011p00685

Fuselier, S. A., Petrinec, S. M., Trattner, K. J., Broll, J. M., Burch, J. L., Giles, B. L., et al. (2018). Observational evidence of large-scale multiple reconnection at the Earth's dayside magnetopause. *Journal of Geophysical Research: Space Physics*, *123*, 8407–8421. https://doi.org/10.1029/2018JA025681

Fuselier, S. A., Petrinec, S. M., Trattner, K. J., & Lavraud, B. (2014). Magnetic field topology for northward IMF reconnection: Ion observations. *Journal of Geophysical Research: Space Physics*, *119*, 9051–9071. https://doi.org/10.1002/2014JA020351

Fuselier, S. A., Trattner, K. J., & Petrinec, S. M. (2011). Antiparallel and component reconnection at the dayside magnetopause. *Journal of Geophysical Research*, *116*, A10227. https://doi.org/10.1029/2011JA016888

Gosling, J. T., Thomsen, M. F., Bame, S. J., Onsager, T. G., & Russell, C. T. (1990). The electron edge of low latitude boundary layer during accelerated flow events. *Geophysical Research Letters*, *17*(11), 1833–1836. https://doi.org/10.1029/GL017i011p01833

Hasegawa, H., Fujimoto, M., Phan, T.-D., Reme, H., Balogh, A., Dunlop, M. W., et al. (2004). Transport of solar wind into Earth's magnetosphere through rolled-up Kelvin-Helmholtz vortices. *Nature*, *430*(7001), 755–758. https://doi.org/10.1038/nature02799

Hasegawa, H., McFadden, J. P., Constantinescu, O. D., Bogdanova, Y. V., Wang, J., Dunlop, M. W., et al. (2009). Boundary layer plasma flows from high-latitude reconnection in the summer hemisphere for northward IMF: THEMIS multi-point observations. *Geophysical Research Letters*, *36*, L15107. https://doi.org/10.1029/2009GL039410

Khotyaintsev, Y. V., Graham, D. B., Norgren, C., Eriksson, E., Li, W., Johlander, A., et al. (2016). Electron jet of asymmetric reconnection. *Geophysical Research Letters*, *43*, 5571–5580. https://doi.org/10.1002/2016GL069064

Le, G., Russell, C. T., Gosling, J. T., & Thomsen, M. F. (1996). ISEE observations of low-latitude boundary layer for northward interplanetary magnetic field: Implications for cusp reconnection. *Journal of Geophysical Research*, *101*(A12), 27,239–27,249. https://doi.org/10.1029/96JA02528

Lv, L. Q., Pu, Z. Y., & Xie, L. (2016). Multiple magnetic topologies in flux transfer events: THEMIS measurements. *Science China Technological Sciences*, *59*(8), 1283–1293. https://doi.org/10.1007/s11431-016-6071-9

Mitchell, D. G., Kutchko, F., Williams, D. J., Eastman, T. E., Frank, L. A., & Russell, C. T. (1987). An extended study of the low-latitude boundary layer on the dawn and dusk flanks of the magnetosphere. *Journal of Geophysical Research*, *92*(A7), 7394–7404. https://doi.org/10.1029/JA092iA07p07394

Ogilvie, K. W., & Fitzenreiter, G. J. (1989). The Kelvin-Helmholtz in- stability at the magnetopause and inner boundary layer surface. *Journal of Geophysical Research*, *94*(A11), 15,113–15,123. https://doi.org/10.1029/JA094iA11p15113

Øieroset, M., Phan, T. D., Gosling, J. T., Fujimoto, M., & Angelopoulos, V. (2015). Electron and ion edges and the associated magnetic topology of the reconnecting magnetopause. *Journal of Geophysical Research: Space Physics*, *120*, 9294–9306. https://doi.org/10.1002/2015JA021580

Phan, T. D., Paschmann, G., & Sonnerup, B. U. Ö. (1996). Low-latitude dayside magnetopause and boundary layer for high magnetic shear: 2. Occurrence of magnetic reconnection. *Journal of Geophysical Research*, *101*(A4), 7817–7828. https://doi.org/10.1029/95JA03751

Pollock, C., Moore, T., Jacques, A., Burch, J., Gliese, U., Saito, Y., et al. (2016). Fast plasma investigation for Magnetospheric Multiscale. *Space Science Reviews*, *199*(1-4), 331–406. https://doi.org/10.1007/s11214-016-0245-4

Pu, Z. Y., Raeder, J., Zhong, J., Bogdanova, Y. V., Dunlop, M., Xiao, C. J., et al. (2013). Magnetic topologies of an in vivo FTE observed by Double Star/TC-1 at Earth's magnetopause. *Geophysical Research Letters*, *40*, 3502–3506. https://doi.org/10.1002/grl.50714

Pu, Z. Y., Zhang, X. G., Wang, X. G., Wang, J., Zhou, X. Z., Dunlop, M. W., et al. (2007). Global view of dayside magnetic reconnection with the dusk-dawn IMF orientation: A statistical study for Double Star and Cluster data. *Geophysical Research Letters*, *34*, L20101. https://doi.org/10.1029/2007GL030336

Russell, C. T., Anderson, B. J., Baumjohann, W., Bromund, K. R., Dearborn, D., Fischer, D., et al. (2016). The Magnetospheric Multiscale magnetometers. *Space Science Reviews*, *199*(1-4), 189–256. https://doi.org/10.1007/s11214-014-0057-3

Sckopke, N., Paschmann, G., Haerendel, G., Sonnerup, B. U. O., Bame, S. J., Forbes, T. G., et al. (1981). Structure of the low-latitude boundary layer. *Journal of Geophysical Research*, *86*(A4), 2099–2110. https://doi.org/10.1029/JA086iA04p02099

Song, P., Elphic, R. C., Russell, C. T., Gosling, J. T., & Cattell, C. A. (1990). Structure and properties of the subsolar magnetopause for northward IMF: ISSE observations. *Journal of Geophysical Research*, *95*(A5), 6375–6387. https://doi.org/10.1029/JA095iA05p06375

Sonnerup, B. U. O. (1974). Magnetopause reconnection rate. *Journal of Geophysical Research*, *79*(10), 1546–1549. https://doi.org/10.1029/JA079i010p01546

Sonnerup, B. U. Ö. (1980). Theory of the low-latitude boundary layer. *Journal of Geophysical Research*, *85*(A5), 2017–2026. https://doi.org/10.1029/JA085iA05p02017

Trattner, K. J., Fuselier, S. A., & Petrinec, S. M. (2004). Location of the reconnection line for northward interplanetary magnetic field. *Journal of Geophysical Research*, *109*, A03219. https://doi.org/10.1029/2003JA009975

Trattner, K. J., Mulcock, J. S., Petrinec, S. M., & Fuselier, S. A. (2007a). Location of the reconnection line at the magnetopause during southward IMF conditions. *Geophysical Research Letters*, *34*, L03108. https://doi.org/10.1029/2006GL028397

Trattner, K. J., Mulcock, J. S., Petrinec, S. M., & Fuselier, S. A. (2007b). Probing the boundary between antiparallel and component reconnection during southward interplanetary magnetic field conditions. *Journal of Geophysical Research*, *112*, A08210. https://doi.org/10.1029/2007JA012270

Trattner, K. J., Petrinec, S. M., Fuselier, S. A., Omidi, N., & Sibeck, D. G. (2012). Evidence of multiple reconnection lines at the magnetopause from cusp observations. *Journal of Geophysical Research*, *117*, A01213. https://doi.org/10.1029/2011JA017080

Trenchi, L., Marcucci, M. F., Pallocchia, G., Consolini, G., Bavassano Cattaneo, M. B., di Lellis, A. M., et al. (2008). Occurrence of reconnection jets at the dayside magnetopause: Double Star observations. *Journal of Geophysical Research*, *113*, A07S10. https://doi.org/10.1029/2007JA012774

Treumann, R. A., LaBelle, J., & Bauer, T. M. (1995). Diffusion processes: An observational perspective. In P. Song, B. U. O. Sonnerup, & M. F. Thomsen (Eds.), *Physics of the Magnetopause*, *Geophysical Monograph Series* (Vol. 90, pp. 331–340). Washington, DC: American Geophysical Union.

Zhang, H., Zong, Q. G., Fritz, T. A., Fu, S. Y., Schaefer, S., Glassmeier, K. H., et al. (2008). Cluster observations of collisionless Hall reconnection at high–latitude magnetopause. *Journal of Geophysical Research*, *113*, A03204. https://doi.org/10.1029/2007JA012769

Zhang, Q.-H., Dunlop, M. W., Lockwood, M., Lavraud, B., Bogdanova, Y. V., Hasegawa, H., et al. (2012). Inner plasma structure of the low-latitude reconnection layer. *Journal of Geophysical Research*, *117*, A08205. https://doi.org/10.1029/2012JA017622

Zhong, J., Pu, Z. Y., Dunlop, M. W., Bogdanova, Y. V., Wang, X. G., Xiao, C. J., et al. (2013). Three-dimensional magnetic flux rope structure formed by multiple sequential X-line reconnection at the magnetopause. *Journal of Geophysical Research: Space Physics*, *118*, 1904–1911. https://doi.org/10.1002/jgra.50281